

Syntheses of New Alternating CT-Type Copolymers of Thiophene and Pyrido[3,4-*b*]pyrazine Units: Their Optical and Electrochemical Properties in Comparison with Similar CT Copolymers of Thiophene with Pyridine and Quinoxaline

Bang-Lin Lee and Takakazu Yamamoto*

Research Laboratory of Resources Utilization, Tokyo Institute of Technology, 4259 Nagatsuta, Midori-ku, Yokohama 226-8503, Japan

Received June 29, 1998; Revised Manuscript Received December 11, 1998

ABSTRACT: Four kinds of new π -conjugated copolymers of electron-donating thiophene with highly electron-withdrawing pyrido[3,4-*b*]pyrazine derivatives have been prepared by using the Stille reaction and electrochemical oxidative polymerization in high yields, and their optical and electrochemical properties have been compared with those of previously reported CT-type π -conjugated polymers. Chemically prepared polymers show an $[\eta]$ value of about 0.3 dL g⁻¹. The π - π^* absorption bands (λ_{max} = ca. 633 nm) of the copolymers are observed at a longer wavelength by about 30 nm than those of similar CT-type copolymers of thiophene with pyridine and quinoxaline. These UV-vis data are considered to reflect a stronger CT interaction between thiophene and pyrido[3,4-*b*]pyrazine, which has a higher electron-withdrawing ability than pyridine and quinoxaline. The copolymers are electrochemically active in both oxidation and reduction regions. In the reduction (n-doping) region, the copolymers show normal three couples of n-doping and n-undoping between -1.55 and -2.25 V vs Ag/Ag⁺. On the other hand, they receive oxidation (p-doping) at E_{pa} of 0.9 V vs Ag/Ag⁺. The electrochemical p- and n-doping of the film of the copolymers is accompanied by changes in its UV-vis spectra (electrochromism), and new absorption bands emerge in the range 900–1500 nm by the p- and n-doping. The X-ray diffraction pattern of the copolymer having a long alkyl side chain suggests self-assembling of the polymer assisted by side chain crystallization.

Introduction

A number of papers have recently been published on the preparation and properties of π -conjugated poly(arylene)s.¹ It is now recognized that the redox behavior of the polymer essentially reflects a basic electronic property of the aromatic unit constituting the polymer,² and various p-type electrically conducting polymers composed of electron-donating aromatic units (e.g., poly(thiophene-2,5-diyl), PTh, poly(pyrrole-2,5-diyl), PPr, and their derivatives) have been prepared; these polymers have already found their practical uses.³

On the other hand, π -conjugated polymers of heteroaromatic compounds containing electron-withdrawing imine nitrogens (e.g., poly(pyridine-2,5-diyl), PPy,⁴ and poly(quinoxaline-2,6-diyl), PQx⁵) are susceptible to reduction (n-doping) and give conducting materials by the reduction.

Recently, a new class of π -conjugated copolymers constituted of both electron-donating and electron-withdrawing heterocyclic units have also been reported,⁶ and these CT-type copolymers show unique optical and electrochemical properties. For example, the copolymers in Chart 1 show their π - π^* absorption band at a longer wavelength than those of the corresponding homopolymers.^{6g}

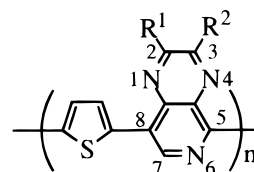
Other types of CT copolymers (e.g., copolymers of thiophene having nitro group and thiophene having alkoxy group) have also been reported.⁷

To obtain further information on these CT-type copolymers, we have prepared new CT-type copolymers

Chart 1. CT-Type Copolymers



of electron-donating thiophene with highly electron-accepting pyrido[3,4-*b*]pyrazine, e.g.,



Pyrido[3,4-*b*]pyrazine and its derivatives have been studied mainly by biochemical interests. They are considered to have a higher electron-accepting ability than pyridine and quinoxaline (e.g., reduction potential vs Hg pool:^{8a} -0.86 V (pyridopyrazine) > -1.10 V (quinoxaline) > -2.20 V (pyridine)) due to their containing three imine nitrogens.⁸ The present research is focused on two properties of the copolymers, i.e., their optical and electrochemical properties, both of which will be affected by the CT structure. Detailed electrochemical analysis has revealed new features of the CT copolymer, and these will also be reported.

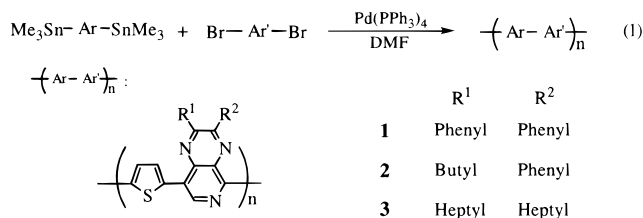
Table 1. Results of the Preparation of Four New Copolymers and Comparison of Their UV-Vis Data with Those of Other Copolymers and a Related Compound

no.	compd	yield, %	$[\eta]^c$, dL g ⁻¹	absorption, λ_{\max} , nm (ϵ , M ⁻¹ cm ⁻¹)	
				in solution ^f	film ^j
1	1 ^a	91	0.27	637 (20 000)	633 660 ^j (on ITO)
2	2 ^a	82		649 (25 000)	657
3	3 ^a	80	0.36	605 (24 000)	<i>k</i>
4	5 ^b				612 ^j
5	7 ^{a,c}	96	0.37	605 (7000)	603
6	8 ^{a,c}	83	0.43	556 (7000)	600
7	9 ^{a,c}	96	0.47	546	<i>k</i>
8	10 ^d	100	2.26	492 (42 000) ^g	475
9	4	93		449 (18 000) ^h	<i>k</i>

^a Prepared by the Stille reaction. ^b Prepared by electrochemical oxidation onto an ITO (indium tin oxide)-coated glass or Pt plate electrode. ^c Data from refs 6g,h. The ϵ value for nos. 5 and 6 was reexamined. ^d Data from refs 6a,c,g. ^e Intrinsic viscosity. Solvent = CF₃COOH for nos. 1 and 3, Cl₂CHCOOH for nos. 5–7, and HCOOH for no. 8. ^f Solvent = CF₃COOH unless otherwise noted. Molarity for the calculation of ϵ is based on the repeating unit (e.g., C₄H₂S–C₁₉H₁₁N₃ for no. 1). ^g Solvent = HCOOH. ^h Solvent = CHCl₃. ⁱ Film formed on a glass substrate by casting unless otherwise noted. ^j On an ITO-coated glass substrate. ^k Good film suited to the optical measurement was not obtained.

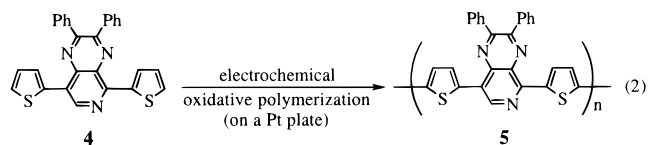
Results and Discussion

Polymerization. Organometallic Polycondensation. The polycondensation (eq 1) using the organometallic reaction⁹ gives the copolymers of thiophene with pyrido[3,4-*b*]pyrazine in high yields as summarized in Table 1.



The copolymers with pyrido[3,4-*b*]pyrazine are soluble in trifluoroacetic acid and dichloroacetic acid and partly soluble in formic acid and chloroform. Polymers **1** and **3** give $[\eta]$ values of 0.27 and 0.36 dL g⁻¹, respectively, in CF₃COOH. The $[\eta]$ values are smaller than that (0.92 dL g⁻¹) of a 1:3 random copolymer of thiophene and pyridine,^{6d,g} which gives a M_w value of 5.1×10^4 in the light scattering analysis. For the present polymers, neither the light scattering analysis nor GPC analysis was possible due to the presence of strong absorption at Ar (488 nm) and He–Ne (632.8 nm) laser positions and due to the absence of solvent suited to the GPC analysis. However, comparison of the $[\eta]$ values of **1** and **3** with that of the 1:3 random copolymer of thiophene and pyridine suggests that the present copolymers have a M_w higher than 1×10^4 . Casting from a HCOOH or CF₃COOH solution followed by treatment with NH₃(aq) and drying recovers the original polymer as proved by IR spectroscopy. Determination of the $[\eta]$ value of **2** was not possible due to its insufficient solubility in solution.

Electrochemical Oxidative Polymerization. Another type of copolymer has also been prepared as a film by an electrochemical oxidative polymerization (eq 2).



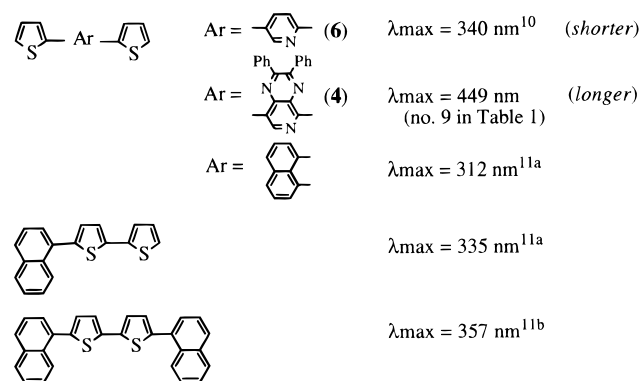
The electrochemical oxidative polymerization of thiophene and its derivatives is known to proceed mainly at the α -position of thiophene, and the IR spectrum of **5** thus obtained resembles the chemically prepared **1** described in eq 1. The polymer **5** was insoluble in solvents including the acidic solvents such as CF₃COOH, possibly due to partial occurrence of cross-linking during the polymerization.

NMR and IR. IR spectra of the copolymers are reasonable for their structures. IR peaks originating from thiophene and pyrido[3,4-*b*]pyrazine units are observed in the range 1400–1500 cm⁻¹; however, the $\nu(\text{C}-\text{Br})$ absorption peaks and the peaks originating from the SnMe₃ group of the monomers are not observable in the IR spectra of the copolymers.

¹H NMR spectra of the copolymers also agree with their structures. The ¹H NMR peaks of **1** are assigned by comparing its ¹H NMR spectrum with those of **4** separately prepared in this work and other related compounds. Figure 1 shows ¹H NMR spectra of **1** and **3** in CF₃COOD. In the part a of Figure 1, a peak at δ 9.37 is assigned to 7-H of the pyrido[3,4-*b*]pyrazine unit, and two broad peaks at δ 8.77 and 8.38 are assigned to the 3- and 4-protons of thiophene rings. The copolymers are considered to contain several microstructures (e.g., head-to-tail (HT) and head-to-head (HH) units), and the peaks seem to have substructures. The signal of the SnMe₃ terminal groups is not observable in the ¹H NMR spectrum.

The ¹H NMR spectrum of **3** (part b of Figure 1) is also reasonable, and the ratios between the signals in Figure 1 agree with the structure of the polymer, indicating that the effect of the terminal groups is small in the NMR spectrum due to a high molecular weight of the copolymer. Figure 2 exhibits the ¹³C CP-MAS solid NMR spectrum of **3**. The NMR spectrum is also consistent with the polymer structure, and tentative assignment of the peaks is given in Figure 2. In CF₃COOD, the ¹³C NMR peaks of **3** are overlapped with peaks of the solvent.

UV-Visible Absorption. Table 1 includes optical data of the copolymers and related compounds. The above shown model compound **4** shows an absorption peak at 449 nm in CHCl₃ (no. 9), which is shifted to a longer wavelength from those of an analogous trimeric compounds, 2,5-bis(2-thienyl)pyridine (340 nm),¹⁰ and related naphthalene-thiophene derivatives.¹¹



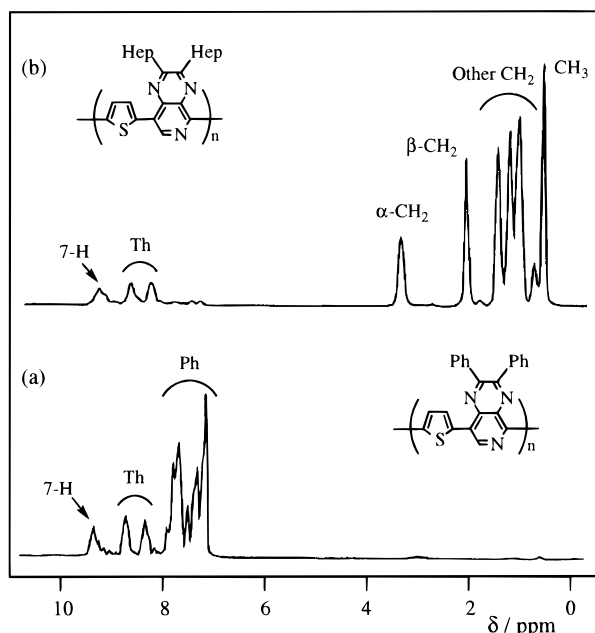


Figure 1. ^1H NMR spectra of (a) **1** and (b) **3** in CF_3COOD .

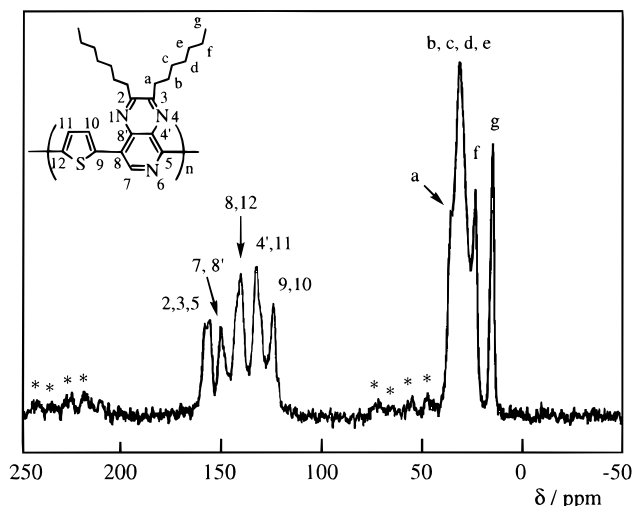
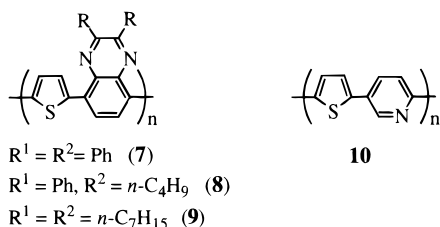


Figure 2. ^{13}C CP-MAS solid NMR spectrum of **3**. The peaks with an asterisk are assigned to spinning sidebands of the aromatic carbon peaks.

Although we have to take into account expansion of the π -system of the central Ar group in changing from **6** to **4**, the data shown above suggest that the appearance of the λ_{max} of **4** at a considerably longer wavelength than that of **6** reflects a higher order of contribution of the CT structure in the electronic state of **4**. The highly charge-transferred structure will lead to a large bathochromic shift of the absorption band.¹²

Figure 3 compares the UV-visible spectrum of a film of **1** with those of the previously reported copolymers,



The data shown in Table 1 and Figure 3 as well as those

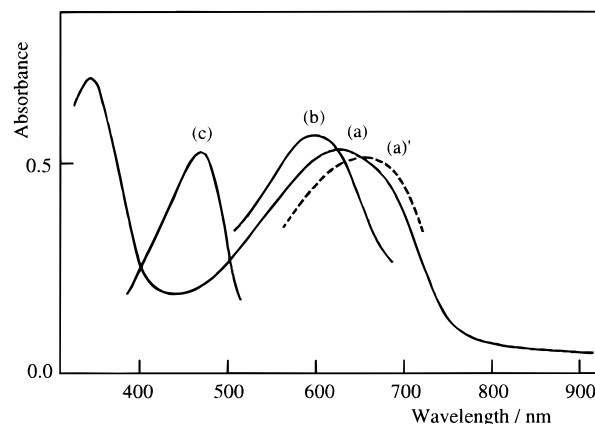
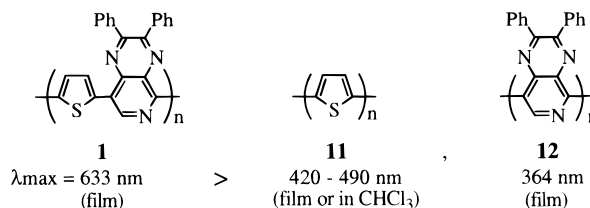


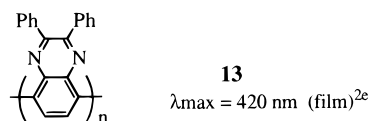
Figure 3. Comparison of UV-visible spectrum of a cast film of **1** (curve a) with those of films of **7** (curve b) and **10** (curve c). (a)–(c): on a quartz glass plate; (a'): a film of **1** on an ITO-coated glass plate.

obtained in separate experiments reveal the following feature of the π - π^* absorption occurring in the copolymers.

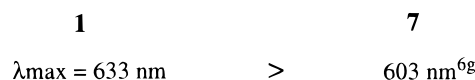
(1) The π - π^* transition of **1** takes place at lower energy than those of the corresponding homopolymers, poly(thiophene-2,5-diyl) (**11**) ($\lambda_{\text{max}} = 420\text{--}490\text{ nm}$)¹³ and poly(2,3-diphenylpyrido[3,4-*b*]pyrazine-5,8-diyl) (**12**) ($\lambda_{\text{max}} = 364\text{ nm}$; cf. Experimental Section).



(2) The homopolymer **12** gives the π - π^* absorption peak at a shorter wavelength than a homopolymer of 2,3-diphenylquinoxaline (**13**) having an analogous π -conjugation system.



However, the copolymer **1** gives rise to the π - π^* absorption peak at a longer wavelength than the corresponding copolymer of 2,3-diphenylquinoxaline.



These data also suggest a higher degree of the contribution of the charge-transferred structure in the electronic state of **1** than in the electronic state of **7**, due to the stronger electron-accepting properties of the pyrido[3,4-*b*]pyrazine unit than the quinoxaline unit.

(3) Other present CT-type polymers (nos. 2–4 in Table 1) also show the π - π^* absorption band at a considerably longer wavelength. By changing the ratio between the two monomeric units from 1:1 (nos. 1–3) to 1:2 (no. 4), the absorption peak seems to move to the direction of the absorption peak of the homopolymer.

(4) The copolymers of pyrido[3,4-*b*]pyrazine (nos. 1–4) and pyridine (no. 8) give a larger ϵ -value than the

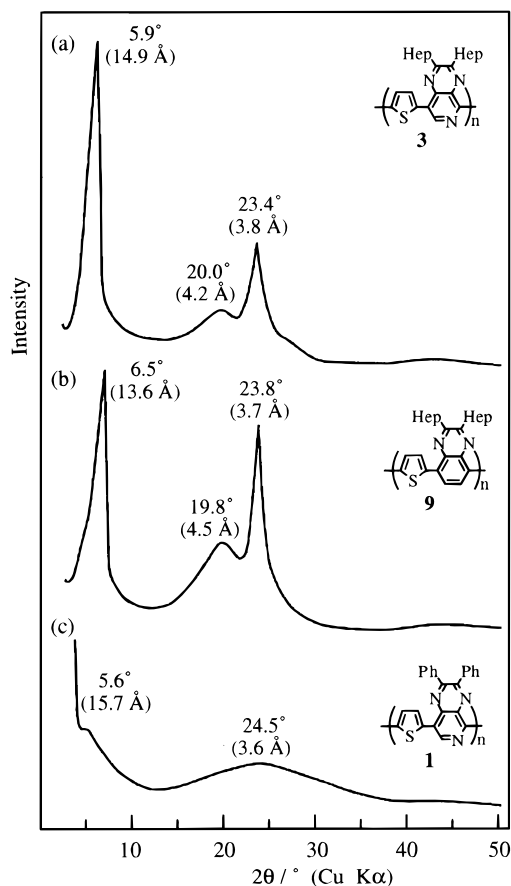
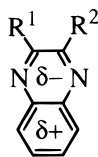


Figure 4. Powder X-ray diffraction patterns of (a) **3**, (b) **9**, and (c) **1**.

copolymers of quinoxaline (nos. 5–7). The reason for such a large difference in ϵ is not clear. However, it may arise from a strongly polarized structure of the quinoxaline unit due to a large difference in the electronegativity between the pyrazine side and benzene ring.



(5) The λ_{\max} position of the film of **1** varies depending on the substrate where the film is laid (no. 1 in Table 1 and charts (a) and (a') in Figure 3). On the glass substrate, the film shows the peak at 633 nm, whereas on an ITO (indium tin oxide) substrate, it gives λ_{\max} at a longer wavelength (660 nm). This phenomenon suggests that the electronic state of the copolymer is affected by the interaction of the copolymer with the surface of the substrate. For example, (a) formation of a special electronic state by interaction of the semiconducting copolymer with n-type conducting ITO and (b) ordering of the copolymer molecules assisted by the interaction with the surface of the substrate are conceivable. However, the ordering of the copolymer molecules, if it takes place, does not seem so extensive as that observed with self-assembled poly(3-alkylthiophene-2,5-diyl) molecules, since self-assembling of the polymer leads to a larger shift of the absorption peak.¹⁴ A similar dependence of λ_{\max} on the kind of the substrates was reported for poly(pyridine-2,5-diyl) and poly(2,2'-bipy-

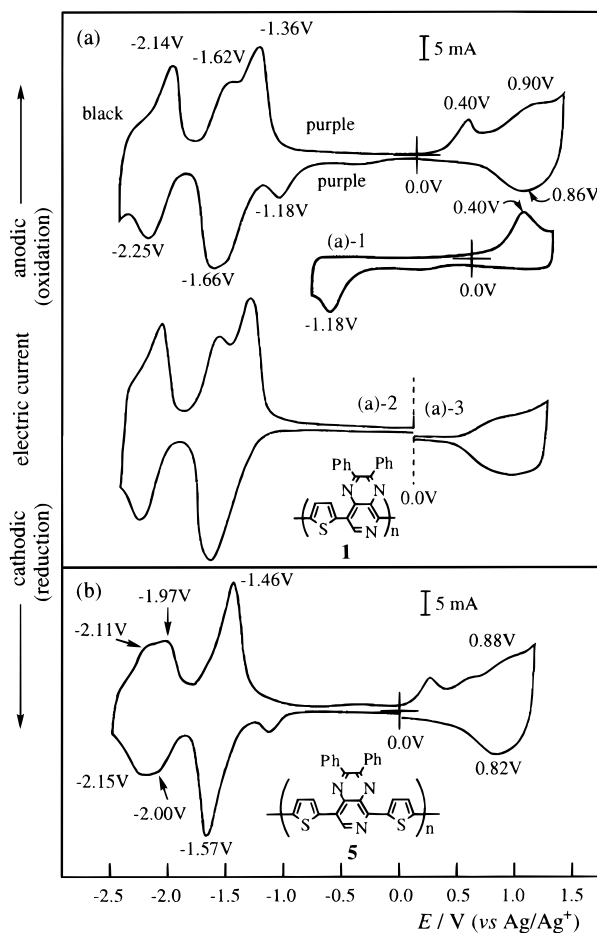


Figure 5. Cyclic voltammograms of films of (a) **1** and (b) **5** on Pt plates (1 cm \times 1 cm) in an CH_3CN solution of $[(\text{C}_2\text{H}_5)_4\text{N}]\text{BF}_4$ (0.1 M) with a sweep range -2.4 to 1.2 V vs Ag/Ag^+ . In a narrow sweep range, the film of **1** gives CV's shown in parts (a)-1 through (a)-3. Sweeping rate = 100 mV s^{-1} .

ridine-5,5'-diyl),¹⁵ and ordering of poly(2,2'-bipyridine-5,5'-diyl) on a glass substrate was also reported.⁴

XRD Pattern. Figure 4 shows XRD patterns of **3**, previously reported **9**, and **1**. As shown in Figure 4, **3** and **9** give analogous XRD patterns to each other, indicating that they take an isomorphous packing in the solid. The strongest peak at $d = 13.6$ or 14.9 \AA is characteristic of polymer materials that form liquid crystal-like phase assisted by side chain crystallization.^{14,16} The d value is considered to correspond to the distance between the main chains of the neighboring two polymer molecules separated by the heptyl group. The molecular model and the number density of the heptyl group along the polymer chain as well as the d value suggest that the polymer molecules take an end-to-end packing mode rather than an interdigitation packing mode.^{14,16,17} In contrast to those two polymers, **1** with the two Ph side groups is essentially amorphous (the part c in Figure 4).

Electrochemical Redox Reaction. Figure 5 exhibits cyclic voltammograms (CV's) of films of the copolymers, **1** and **5**, laid on Pt plates.

As shown in Figure 5, **1** and **5** give rise to electrochemical redox cycles in both oxidation and reduction regions, similar to the previously reported CT-type copolymers, **7–10**.^{6a,g}

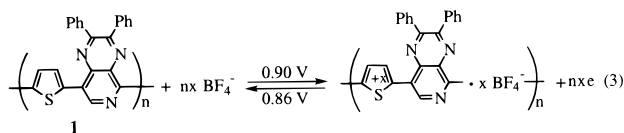
Table 2. CV Data of the Copolymers and Model Compounds (Nos. 7 and 8)

no.	compd	redox potential, V vs Ag/Ag ⁺ ^a		<i>E</i> ^b /V	redox potential, V vs Ag/Ag ⁺ ^a		<i>E</i> ^b /V
		p-doping (<i>E</i> _{pa})	p-undoping (<i>E</i> _{pc})		n-doping (<i>E</i> _{pc})	n-undoping (<i>E</i> _{pa})	
1	1	0.90	0.86	0.88	-1.66 -1.66 -2.25	-1.36 -1.62 -2.14	-1.51 -1.64 -2.20
2	2	0.90	0.80	0.85	-1.18 -1.69 -1.86	0.40 -1.49 -1.77	$\Delta E = 1.58$ -1.43 -1.82
3	3	0.90	0.82	0.86	-2.21 -1.20 -1.79	-2.26 0.38 -1.63	$\Delta E = 1.58$ -1.71 -1.88
4	5^c	0.88	0.82	0.85	-1.93 -2.40 -1.20	-1.85 -2.32 0.39	-2.36 $\Delta E = 1.59$ -1.52
5	7^d	0.64	0.60	0.62	-2.00 ^f -2.15 ^f -1.08	-1.97 ^f -2.11 ^f 0.21	-1.99 -2.13 $\Delta E = 1.29$
6	10^d	0.96	0.86	0.91	-1.80 -1.94 -2.20	-1.60 -1.85 -2.02	-1.70 -1.90 -2.11
7	4^e	0.91	0.55	0.73	-1.70 -2.16 -1.54	0.40 -2.10 -1.48	$\Delta E = 2.10$ -2.13 -1.51
8	8^e				-1.77 -2.54	-1.69 -2.26	-1.73 -2.40

^a Measured in an acetonitrile solution of [(C₂H₅)₄N]BF₄ (0.1 M). *E*_{pa} = peak anode potential; *E*_{pc} = peak cathodic potential. For nos. 1–3, 5, and 6, the data were obtained with polymer films laid on a Pt plate. For nos. 7 and 8, solutions of the model compounds were used. ^b The average of *E*_{pa} of *E*_{pc} is given. ^c Measured with film grown on ITO glass electrode by electrochemical oxidation. ^d Data from refs 6a,c,g. Additional data obtained by scanning up to 1.0 V vs Ag/Ag⁺ (cf. the text and ref 20) are added. ^e Measured with an acetonitrile solution of **4** or 2,3-diphenylpyrido[3,4-*b*]pyrazine. ^f Broad and overlapped peak. ^g 2,3-Diphenylpyrido[3,4-*b*]pyrazine.

Electrochemical Oxidation (p-Type Doping). The polymer **1** shows a main p-doping (or oxidation) peak at 0.90 V and its coupled broad p-undoping peak at 0.86 V. The p-doping and p-undoping CV pattern is similar to that observed for electrochemical redox reactions of the thiophene unit in polythiophene.¹ However, the oxidation of thiophene ring in **1** requires a higher potential than those of polythiophene in agreement with the attachment of the electron-withdrawing pyrido[3,4-*b*]pyrazine units.¹⁸ The p-doping process of the polymer can be expressed by the following equation.

p-Doping :

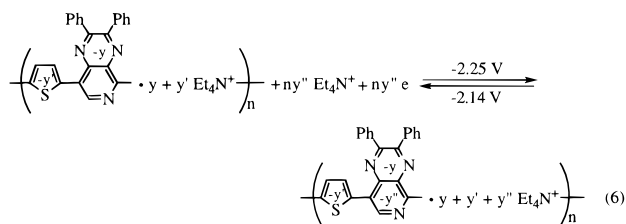
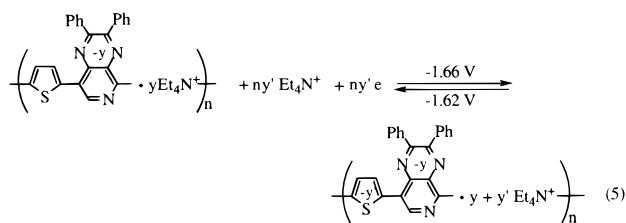
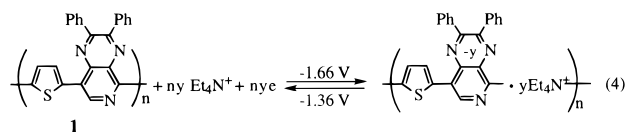


The doping level (*x* in eq 3) estimated from the electric current was 0.32.

In the oxidation region, there is observed another oxidation peak at 0.4 V; in the reduction, below 0 V vs Ag/Ag⁺, several redox peaks are observed, and these peaks are discussed below. Table 2 summarizes the CV data of the copolymers and related compounds.

Electrochemical Reduction (n-Doping). As shown in Figure 5, the CV chart of **1** exhibits n-doping peaks at -1.66 and -2.25 V vs Ag/Ag⁺. The former reduction peak is coupled with the oxidation peak at -1.36 and -1.62 V, whereas the latter to the oxidation peak at -2.14 V vs Ag/Ag⁺. Since the reduction peak area at -1.66 V agrees with the sum of the oxidation peak areas at -1.62 and -1.36 V, two reduction peaks are considered to be overlapped to give the apparently single reduction peak at -1.66 V vs Ag/Ag⁺. On the basis of these results, **1** is assumed to receive the three-step reduction shown in eqs 4–6).

n-Doping :



The first step reduction of **1** is considered to occur mainly at the pyridopyrazine ring (eq 4), since pyridopyrazine has the highly electron-accepting property. The injected negative charge will mainly locate at the pyrazine moiety of the pyridopyrazine ring due to its containing two electron-withdrawing imine nitrogens;¹⁹ however, of course, the negative charge is considered to be delocalized along the polymer chain. The second reduction is considered to occur at the thiophene ring (eq 5), because the pyrido[3,4-*b*]pyrazine unit has already accepted the negative charge. The last reduction is considered to take place by injection of additional negative charge into the pyrido[3,4-*b*]pyrazine unit

(presumably mainly at the pyridine moiety; eq 6). The above-described assignment of the three reduction peaks is consistent with CV data of monomeric 2,3-diphenylpyrido[3,4-*b*]pyrazine (no. 8 in Table 2). The total negative charge ($y + y' + y''$) thus stored by the repeating unit is estimated at 1.80, which corresponds to 480 C/(1 g of the polymer) or 130 W h kg⁻¹. The polymer **5** electrochemically prepared also gives analogous p-doping and n-doping peaks (part b in Figure 5 and no. 4 in Table 2).

Reversible Prepeaks Observed at -1.18 and 0.40 V. The CV chart of **1** (part a in Figure 5) shows another redox couple (or prepeaks) with E_{pc} at -1.18 V and E_{pa} at 0.40 V vs Ag/Ag⁺. Other present copolymers of thiophene and pyrido[3,4-*b*]pyrazine as well as previously reported copolymers of thiophene and pyridine (e.g., the polymer **10**)^{6a,g,20} give rise to an analogous redox couple. Investigation of the prepeaks gives the following results.

(1) CV data obtained with narrower scanning range (parts (a)-1 through (a)-3 in Figure 5) clearly indicate the coupling of the E_{pc} peak at -1.18 V with the E_{pa} peak at 0.40 V.

(2) This couple is observed only after the polymer is scanned at least once beyond both 0.40 and -1.18 V. Namely, this couple is not observed at the first CV cycle, regardless of the scanning direction to the oxidation or reduction. The couple is observed only after the second CV cycle.

(3) The copolymers of thiophene with pyridine and pyrido[3,4-*b*]pyrazine afford such a couple (or the prepeaks), whereas the copolymers of thiophene and quinoxaline (cf. Chart 1) do not show the couple. These results suggest the importance of the presence of a nitrogen atom in the main-chain ring (not in the side-chain ring) of the electron-accepting aromatic unit of the copolymer for the prepeaks.

(4) The trimeric model compound **4** in an acetonitrile solution of [NEt₄]BF₄ does not show such a reversible prepeaks, suggesting that they are characteristic of the solid system.

(5) Use of an ITO (indium tin oxide) electrode for the polymer, instead of the Pt electrode, also gives the prepeaks.

For the reversible prepeaks, we do not have a clear-cut explanation at the moment. However, conformational changes of the copolymer caused by oxidation beyond 0.40 V and reduction beyond -1.18 V vs Ag/Ag⁺ may bring about such a large difference ($\Delta E = 1.6$ V; cf. Table 2) between the oxidation and reduction potentials. Two research groups have reported similar prepeaks for polythiophene and poly(bithiophene),²¹ and the peaks are attributed to the occurrence of chemical reaction(s) on the thiophene ring. If a similar explanation can be applied, the present results suggest the importance of cooperation of the thiophene ring and pyridine ring for the chemical reaction(s) (e.g., chelating trap of cation dopant by the thiophene and pyridine units).

Electrochromism. Figure 6 depicts UV-visible absorption spectra of film cast on an ITO during the electrochemical p- and n-doping.

p-Doping. At 0.0 V vs Ag/Ag⁺, the nondoped **1** film gives rise to π - π^* absorption bands at 350 and 660 nm. On the application of the oxidation potential, these two absorption bands, especially the one at 660 nm assigned to the π - π^* transition occurring mainly along the polymer chain, become weaker, and new absorption

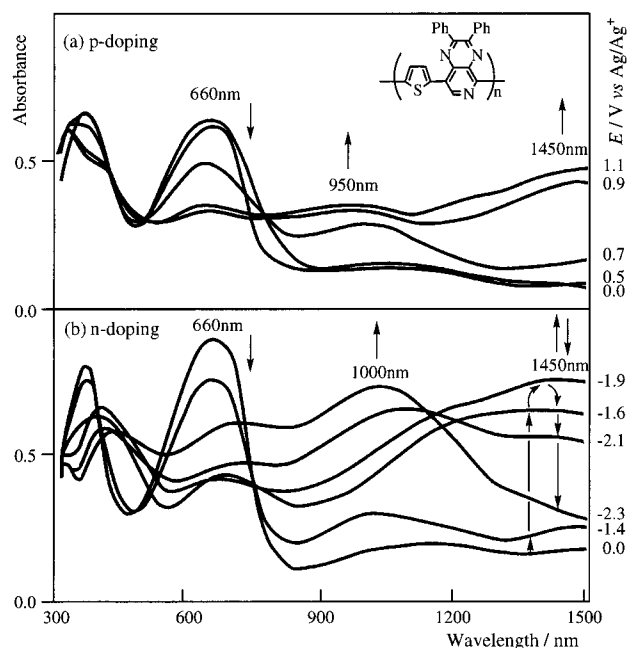


Figure 6. Changes in the absorption spectrum of a film of **1** on an ITO electrode during electrochemical (a) p-doping and (n) n-doping in an CH₃CN solution of [(C₂H₅)₄N]BF₄ (0.1 M).

bands at about 950 and 1450 nm emerge. These two new absorption bands are characteristic of oxidized poly(arylene)s such as poly(thiophene). At a lower oxidation potential, e.g., at 0.7 V, the degree of oxidation will be lower, and this state gives the peak at 950 nm, whereas at 1.1 V where more extensive oxidation takes place the absorption peak at 1450 nm becomes stronger. These results suggest that the absorption band at 950 nm observed at the lightly oxidized state originates from a so-called polaron oxidized state, and the absorption band at 1450 nm originates from a so-called bipolaron oxidized state formed by coupling of the two polarons.¹

n-Doping. As shown in the part b in Figure 6, the reduction of the polymer also leads to great change in the UV-vis spectrum, similar to cases of reduction of electron-accepting poly(arylene)s.^{2d,22} Usual electron-accepting poly(arylene)s such as poly(quinoline)s, however, cause rather simple UV-vis changes, i.e., a continuous increase in the intensity of the new absorption band in the range 900–1500 nm by applying more negative potential. In contrast to those cases, the UV-vis spectrum of the present polymer exhibits a complicated change depending on the applied voltage, due to the presence of multiple centers to accept the electron. As for the peak at 1450 nm, its intensity initially increases with the increase in the negatively applied potential; however, it decreases on further increase in the negatively applied potential. In the case of the peak at 1000 nm, however, its intensity continuously increases with the negatively applied potential.

Electrical Conductivity. The present CT copolymers themselves show only low electrical conductivities σ of below 10⁻⁸ S cm⁻¹. The iodine-doped **1** shows an electrical conductivity of 1.0 × 10⁻⁶ S cm⁻¹.

Conclusions

A series of π -conjugated CT-type copolymers of thiophene with pyrido[3,4-*b*]pyrazine have been prepared by the organometallic polycondensation and the electrochemical polymerization. The copolymers are

soluble in CF_3COOH and Cl_2CHCOOH and partly soluble in HCOOH and CHCl_3 . UV-visible absorption peaks of the copolymers in solution and films appear at a longer wavelength compared with those of the corresponding homopolymers, and the degree of the bathochromic shift is larger than those observed with the previously reported analogous copolymers of thiophene with pyridine and quinoxaline. These data reflect the strongly electron-accepting property of the pyrido[3,4-*b*]pyrazine unit. The copolymers are electrochemically active in both the reduction and oxidation regions. In the reduction region, the CV chart exhibits three-step reductions (n-doping), which are ascribed to the reduction at the pyrazine, thiophene, and pyridine ring in the copolymer. The oxidation and reduction of the copolymers are accompanied by changes of colors (electrochromism).

Experimental Section

Materials and Measurements. Solvents were dried, distilled, and stored under N_2 . ^1H NMR and IR spectra were recorded on a JEOL EX-400 spectrometer and a JASCO IR-810 spectrometer, respectively. UV-visible absorption spectra were reported on a Shimadzu UV-3100 spectrometer. Electrochemical polymerization and cyclic voltammetry were performed with a Hokuto Denko HA-501 galvanostat/potentiostat and a Hokuto Denko KB-104 function generator.

Polymerization. Preparation of the copolymers was carried out by using the Stille reaction^{6h,9} or electrochemical oxidation. The homopolymer **12** was prepared by using a Ni(0) complex.^{6g} Details of the preparation of **1**, **5**, and **12** as well as analytical and spectroscopic data of the polymers are shown below.

Polymer 1. 2,5-Bis(trimethylstannyl)thiophene (0.41 g, 1.00 mmol) and 5,8-dibromo-2,3-diphenylpyrido[3,4-*b*]pyrazine (0.44 g, 1.00 mmol) were dissolved in dry DMF (20 mL) under N_2 atmosphere. To the solution was added $\text{Pd}(\text{PPh}_3)_4$ (57.8 mg, 0.05 mmol) and stirred at 80 °C for 48 h. After cooling, a precipitate of the dark purple copolymer was separated by filtration and washed with methanol, a dilute HCl aqueous solution, dilute ammonia, and acetone in this order. Thus, a dark purple powder of copolymer **1** was obtained (0.33 g, yield = 91%). Anal. Calcd for $(\text{C}_{25}\text{H}_{13}\text{N}_3\text{S} \cdot 0.7\text{H}_2\text{O})_n$: C, 73.5; H, 3.9; N, 11.1; S, 8.5; Br, 0.0. Found: C, 73.5; H, 3.6; N, 10.9; S, 8.0; Br, 0.6. IR (KBr, cm^{-1}): 3054, 1521, 1445, 1407, 1375, 1305, 1228, 976, 767, 693, 538. ^1H NMR (CF_3COOD , ppm): 7.71–7.96 (b, 10H, phenyl), 8.38 (b, 1H, thienyl), 8.77 (b, 1H, thienyl), 9.37 (s, 1H, pyrido[3,4-*b*]pyrazine). $[\eta] = 0.27 \text{ dL g}^{-1}$ in CF_3COOH at 30 °C.

Preparation of other CT type copolymers was carried out analogously.

Polymer 2. Dark purple powders. Yield = 82%. Anal. Calcd for $(\text{C}_{21}\text{H}_{17}\text{N}_3\text{S} \cdot 0.3\text{H}_2\text{O})_n$: C, 72.4; H, 5.1; N, 12.0; S, 9.2; Br, 0.0. Found: C, 72.0; H, 4.7; N, 11.6; S, 8.8; Br, 0.0. IR (KBr, cm^{-1}): 3048, 2954, 2856, 1522, 1443, 1412, 1375, 1333, 1217, 1003, 694, 497. ^1H NMR (CF_3COOD , ppm): 0.64–2.06 (m, 7H, butyl), 2.96 and 3.63 (m, 2H, CH_2), 7.32–8.00 (m, 5H, phenyl), 8.29 (b, 1H, thienyl), 8.69 (b, 1H, thienyl), 9.26 (b, 1H, pyrido[3,4-*b*]pyrazine).

Polymer 3. Dark purple powders. Yield = 80%. Anal. Calcd for $(\text{C}_{25}\text{H}_{33}\text{N}_3\text{S} \cdot 0.4\text{H}_2\text{O})_n$: C, 72.4; H, 8.2; N, 10.1; S, 7.7; Br, 0.0. Found: C, 72.1; H, 7.8; N, 10.0; S, 7.7; Br, 0.0. IR (KBr, cm^{-1}): 3048, 2924, 2852, 1523, 1465, 1428, 1334, 1281, 1148, 817, 503. ^1H NMR (CF_3COOD , ppm): 0.74 (b, 6H, CH_3), 0.91–2.22 (m, 20H, $(\text{CH}_2)_5$), 3.49 (b, 4H, CH_2), 8.30 (b, 1H, thienyl), 8.64 (b, 1H, thienyl), 9.26 (b, 1H, pyrido[3,4-*b*]pyrazine). CP MAS ^{13}C NMR: δ 158.8, 157.3, 156.3, 150.9, 141.5, 133.6, 124.7. $[\eta] = 0.36 \text{ dL g}^{-1}$ in CF_3COOH at 30 °C.

Polymer 5. The electrochemical polymerization was carried out in a CV cell with two compartments equipped with three electrodes [Pt disk working electrode, Pt wire counter electrode, and a Ag/Ag^+ (0.1 M in an CH_3CN solution (0.1 M) of $[(\text{C}_2\text{H}_5)_4\text{N}]\text{BF}_4$) reference electrode] system. The polymer film

was grown on a Pt plate or ITO-coated glass electrode in an CH_3CN solution containing the monomer, **4** ($2.1 \times 10^{-4} \text{ M}$), and 0.1 M $[(\text{C}_2\text{H}_5)_4\text{N}]\text{BF}_4$ by repetitive scan from 0.0 to +0.98 V vs Ag/Ag^+ at 100 mV s^{-1} . The dark purple film was rinsed with CH_3CN and dried for analysis, whereas the as-grown polymer film was used for the CV measurements.

Homopolymer 12. Stirring a mixture of bis(1,5-cyclooctadiene)nickel ($\text{Ni}(\text{cod})_2$) (0.55 g, 1.95 mmol), 1,5-cyclooctadiene (0.37 mL), 2,2'-bipyridyl (0.32 g, 2.0 mmol), and 5,8-dibromo-2,3-diphenylpyrido[3,4-*b*]pyrazine (0.66 g, 1.50 mmol) in DMF (20 mL) for 48 h at 60 °C afforded a precipitate of the homopolymer. The precipitate was washed with $\text{NH}_4\text{OH}(\text{aq})$, an aqueous solution of disodium ethylenediaminetetraacetic acid (Na_2EDTA), warm water, and acetone, in this order, and dried under vacuum to obtain a powder of **12** (yield = 81%). Anal. Calcd for $(\text{C}_{19}\text{H}_{11}\text{N}_3 \cdot 1.2\text{H}_2\text{O})_n$: C, 75.3; H, 4.5; N, 13.9; Br, 0.0. Found: C, 75.1; H, 4.1; N, 13.6; Br, 0.0.

Acknowledgment. This work has been partly supported by a Research Fellowships of the Japan Society for the Promotion of Science for Young Scientists (JSPS Research Fellowships for the Promotion of Science for Young Scientists), a Grant-in-Aid for Science Research from the Ministry of Education, Science, Sports, and Culture, and CREST (Core Research for Evolutional Science and Technology).

Supporting Information Available: Scheme for synthesis of 5,8-dibromopyrido[3,4-*b*]pyrazine derivatives (S-1), synthesis of 3,4-diamino-2,5-dibromopyridine (S-2), synthesis of 5,8-dibromopyrido[3,4-*b*]pyrazine (S-3), and synthetic data of trimeric compound (**4**) (S-4). This material is available free of charge via the Internet at <http://pubs.acs.org>.

References and Notes

- (1) (a) Skotheim, T. A., Ed. *Handbook of Conducting Polymers*; Marcel Dekker: New York, 1986; Vols. I and II. (b) Nalwa, H. S., Ed. *Handbook of Organic Conductive Molecules and Polymers*; John Wiley: New York, 1997. (c) Skotheim, T. A., Elsenbaumer, R. L., Reynolds, J. R., Eds. *Handbook of Conducting Polymers*, 2nd ed.; Marcel Dekker: New York, 1997. (d) Salaneck, W. R.; Clark, D. T.; Samuelsen, E. J. *Science and Applications of Conducting Polymers*; Adam Hilger: Bristol, 1991.
- (2) (a) Kanbara, T.; Yamamoto, T. *Macromolecules* **1993**, *26*, 1975. (b) Yamamoto, T. *J. Polym. Soc., Part A: Polym. Chem.* **1996**, *34*, 997. (c) Yamamoto, T. *Proc. Polym. Sci.* **1992**, *17*, 1153. (d) Agrawal, A. K.; Jenekhe, S. A. *Chem. Mater.* **1996**, *8*, 579. (e) Yamamoto, T.; Sugiyama, K.; Kushida, T.; Inoue, T.; Kanbara, T. *J. Am. Chem. Soc.* **1996**, *118*, 3930. (f) Mackintosh, J. G.; Mount, A. R. *J. Chem. Soc., Faraday Trans.* **1994**, *90*, 1121. (g) Faid, K.; Leclerc, M.; Nguyen, M.; Diaz, A. *Macromolecules* **1995**, *28*, 284.
- (3) For example: (a) Kudoh, Y.; Fukuyama, M.; Kojima, T.; Nanai, N.; Yoshimura, S. In *Intrinsically Conducting Polymers: An Emerging Technology*; Mldissi, M., Ed.; Kluwer Academic Publishers: Dordrecht, 1993. (b) Kudoh, Y.; Kojima, T.; Fukuyama, M.; Tsuchiya, S.; Yoshimura, S. *J. Power Sources* **1996**, *60*, 157. (c) Leeuw, D. M.; Kraakman, P. A.; Bongaerts, P. F. G.; Mutsaers, C. M. J. *Synth. Met.* **1994**, *66*, 263. (d) Jonas, F.; Heywang, G. *Electrochim. Acta* **1994**, *39*, 1345. (e) Tomozawa, H.; Ikenoue, Y.; Murai, F.; Suzuki, Y.; Towa, T.; Ohta, Y. *J. Photopolym. Sci. Technol.* **1996**, *9*, 707.
- (4) Yamamoto, T.; Maruyama, T.; Zhou, Z.-H.; Ito, T.; Fukuda, T.; Yoneda, Y.; Begum, F.; Ikeda, T.; Sasaki, S.; Takezoe, H.; Fukuda, A.; Kubota, K. *J. Am. Chem. Soc.* **1994**, *116*, 4832.
- (5) Saito, N.; Kanbara, T.; Kushida, T.; Kubota, K.; Yamamoto, T. *Chem. Lett.* **1993**, 1775.
- (6) (a) Zhou, Z.-H.; Maruyama, T.; Kanbara, T.; Ikeda, T.; Ichimura, K.; Yamamoto, T.; Tokuda, K. *J. Chem. Soc., Chem. Commun.* **1991**, 1210. (b) Ferraris, J. P.; Bravo, A.; Kim, W.; Hrnčir, D. C. *J. Chem. Soc., Chem. Commun.* **1994**, 991. (c) Yamamoto, T.; Zhou, Z.-H.; Maruyama, T. *Synth. Met.* **1993**, *55/57*, 1209. (d) Yamamoto, T.; Shimura, M.; Osakada, K.; Kubota, K. *Chem. Lett.* **1992**, 1003. (e) Higgins, S.; Crayston, J. A. *Synth. Met.* **1993**, *55/57*, 879. (f) Karikomi, M.; Kitamura, C.; Tanaka, S.; Yamashita, Y. *J. Am. Chem. Soc.* **1995**,

- 117, 6791. (g) Yamamoto, T.; Zhou, Z.-H.; Kanbara, T.; Shimura, M.; Kizu, K.; Maruyama, T.; Nakamura, Y.; Fukuda, T.; Lee, B.-L.; Ooba, N.; Tomaru, S.; Kurihara, T.; Kaino, T.; Kubota, K.; Sasaki, S. *J. Am. Chem. Soc.* **1996**, *118*, 10389. (h) Kanbara, T.; Miyazaki, Y.; Yamamoto, T. *J. Polym. Soc., Part A: Polym. Chem.* **1995**, *33*, 999.
- (7) (a) Demanze, F.; Yassar, A.; Garnier, F. *Macromolecules* **1996**, *29*, 4267. (b) Zhang, Q. T.; Tour, J. M. *J. Am. Chem. Soc.* **1997**, *119*, 5065. (c) Zhang, Q. T.; Tour, J. M. *J. Am. Chem. Soc.* **1998**, *120*, 5355. (d) Hung, H.; Pickup, P. G. *Chem. Mater.* **1998**, *10*, 2212.
- (8) (a) Wiberg, K. B.; Lewis, T. P. *J. Am. Chem. Soc.* **1970**, *92*, 7154. (b) Dillow, G. W.; Kebarle, P. *Can. J. Chem.* **1989**, *67*, 1628.
- (9) (a) Still, J. K. *Angew. Chem.* **1986**, *98*, 504; *Angew. Chem., Int. Ed. Engl.* **1986**, *25*, 508. (b) Kosugi, M.; Koshiha, M.; Sano, H.; Migita, T. *Bull. Chem. Soc. Jpn.* **1985**, *58*, 1075. (c) Bochmann, M.; Kelly, K. *J. Chem. Soc., Chem. Commun.* **1989**, 532. (d) Echavarren, A. M.; Stille, J. K. *J. Am. Chem. Soc.* **1987**, *109*, 5478. (e) Bao, Z.; Chan, W.; Yu, L. *Chem. Mater.* **1993**, *5*, 2; *J. Am. Chem. Soc.* **1995**, *117*, 12426.
- (10) Sease, J. W.; Zechmeister, L. *J. Chem. Soc.* **1947**, 69, 270.
- (11) (a) Kuroda, M.; Nakayama, J.; Hoshino, M.; Furusho, N. *Tetrahedron Lett.* **1992**, *33*, 7553. (b) Kuroda, M.; Nakayama, J.; Hoshino, M.; Furusho, N.; Ohba, S. *Tetrahedron Lett.* **1994**, *35*, 3957.
- (12) Briegleb, G. *Elektronen-Donator-Acceptor-Komplexe*; Springer: Berlin, 1961.
- (13) (a) Yamamoto, T.; Sanechika, K.; Yamamoto, A. *Bull. Chem. Soc. Jpn.* **1983**, *56*, 1497. (b) Tourillon, G. In *Handbook of Conducting Polymers*; Skotheim, T. A., Ed.; Marcel Dekker: New York, 1986; Vol. 2, p 293.
- (14) (a) McCullough, R. D.; Tristram-Nagle, S.; Williams, S. P.; Lowe, R. D.; Jayaraman, M. *J. Am. Chem. Soc.* **1993**, *115*, 4910. (b) Chen, T.-A.; Wu, X.; Rieke, R. D. *J. Am. Chem. Soc.* **1995**, *117*, 233. (c) Yamamoto, T.; Komarudin, D.; Arai, M.; Lee, B.-L.; Suganuma, H.; Asakawa, N.; Inoue, Y.; Kubota, K.; Sasaki, S.; Fukuda, T.; Matsuda, H. *J. Am. Chem. Soc.* **1998**, *120*, 2047 and references therein.
- (15) Yamamoto, T.; Maruyama, T.; Ikeda, T.; Sisido, M. *J. Chem. Soc., Chem. Commun.* **1990**, 1306.
- (16) (a) Jordan, E. F., Jr.; Feldeisen, D. W.; Wrigley, A. N. *J. Polym. Soc., Part A-1* **1971**, *9*, 1835. (b) Hsieh, H. W.; Post, B.; Morawetz, H. *J. Polym. Soc., Polym. Phys. Ed.* **1976**, *14*, 1241. (c) Nagao, M.; Sasaki, S.; Hayashi, T.; Uematsu, I. *Polym. Bull.* **1983**, *9*, 11. (d) Watanabe, J.; Harkness, B. R.; Sone, M.; Ichimura, H. *Macromolecules* **1994**, *27*, 507.
- (17) Polymers **3** and **9** have densities of 1.26 and 1.28 g cm⁻³ as measured with a float-sink method.
- (18) (a) Zhu, S. S.; Swager, T. M. *Adv. Mater.* **1996**, *8*, 497. (b) Jenkins, I. H.; Salzner, U.; Pickup, P. G. *Chem. Mater.* **1996**, *8*, 2444.
- (19) Pyrazine, pyridine, and thiophene themselves have the reduction potential of 0.4, -0.62, and -1.15 eV, respectively (ref 6g and Nenner, I.; Schulz, G. T. *J. Chem. Phys.* **1975**, *62*, 1747).
- (20) In our previous work,^{6a,g} CV was carried out in a potential range below 0.50 V vs Ag/Ag⁺, and we assigned the oxidation peak of the copolymer of Th and Py (PThPy) observed at 0.40 V to the p-doping of the thiophene unit. However, scanning up to 1.20 V gives rise to a new redox cycle with E_{pa} of 0.96 V and E_{pc} of 0.86 V, similar to cases of the present copolymers (cf. text, Figure 5, and no. 6 in Table 2), and the new redox cycle is now associated with the p-doping and p-undoping. The redox couple of PThPy with E_{pc} of -1.70 V and E_{pa} of 0.40 V is discussed in the text.
- (21) (a) Borjas, R.; Buttry, D. A. *Chem. Mater.* **1991**, *3*, 872. (b) Zotti, G.; Schiavon, G.; Zecchin, S. *Synth. Met.* **1995**, *72*, 275.
- (22) (a) Saito, N.; Yamamoto, T. *Macromolecules* **1995**, *28*, 4260. (b) Yamamoto, T.; Suganuma, H.; Maruyama, T.; Inoue, T.; Muramatsu, Y.; Arai, M.; Komarudin, D.; Ooba, N.; Tomaru, S.; Sasaki, S.; Kubota, K. *Chem. Mater.* **1997**, *9*, 1217.

MA9810130